

## Adsorption and Corrosion Inhibition Performance of 2-(*p*-bromobenzylthio)-1*H*-benzimidazole for Q235 Steel in HCl Solution

Chuan Lai<sup>1,2</sup>, Hongxia Yang<sup>2</sup>, Xiaogang Guo<sup>3</sup>, Xiulan Su<sup>1</sup>, Lvshan Zhou<sup>1</sup>, Lei Zhang<sup>1</sup>, Bin Xie<sup>2,\*</sup>

<sup>1</sup> School of Chemistry and Chemical Engineering, Sichuan University of Arts and Science, Dazhou 635000, PR China

<sup>2</sup> Institute of Functional Materials, School of Chemical and Environmental Engineering, Material Corrosion and Protection Key Laboratory of Sichuan Province, Sichuan University of Science and Engineering, Zigong 643000, PR China

<sup>3</sup> College of Chemistry and Chemical Engineering, Chongqing University, Chongqing 400044, PR China

\*E-mail: [xiebinsuse@163.com](mailto:xiebinsuse@163.com)

Received: 20 September 2016 / Accepted: 28 October 2016 / Published: 10 November 2016

---

The new organic corrosion inhibitor of 2-(*p*-bromobenzylthio)-1*H*-benzimidazole (Br-BBD) was synthesized in this work. After prepared, the adsorption and corrosion inhibition performance of Br-BBD for Q235 steel in HCl solution were studied using EIS, SEM, polarization measurement and WLM (weight loss measurement). The results exhibit that Br-BBD acts as an excellent corrosion inhibitor for Q235 steel in HCl solution, and the inhibition efficiency can reach up to 98.07% when the Br-BBD concentration is 50 mg L<sup>-1</sup> in 1.0 M HCl at 25°C. In addition, the adsorption of the mixed-type inhibitor of Br-BBD on Q235 steel surface obey Langmuir adsorption isotherm, which is governed by spontaneous chemisorption mechanism.

---

**Keywords:** Adsorption; Corrosion inhibitor; Q235 steel; 2-mercaptobenzimidazole.

### 1. INTRODUCTION

Corrosion of metals has been the subject of many studies, particularly in acidic environments commonly in several industrial fields. The damage by metals, alloys materials and their equipment corrosion not only generates high cost for inspection, repairing and replacement, but constitutes a public risk. Using corrosion inhibitors for prevention is one of an effective method for corrosion prevention by metals and alloys materials corrosion in acidic environments, for removing scales and

rusts in metal finishing industries, cleaning of boilers and heat exchangers [1-4]. At present, several organic compounds have been evaluated as corrosion inhibitor for metal protection in corrosive media. Based on previous works [5-9], it can be found that 2-mercaptobenzimidazole can act as corrosion inhibitor, and the corrosion inhibition of this inhibitor for different metals and alloys in acid media including  $\text{H}_2\text{SO}_4$ ,  $\text{HCl}$ ,  $\text{H}_3\text{PO}_4$  was systematic studied and evaluated. However, there have been a few reports about the derivatives of 2-mercaptobenzimidazole using as corrosion inhibitor. It is well known that the efficiency of organic corrosion inhibitor is mainly due to the physical and/or chemical adsorption resulting from the interaction of polar centers of the inhibitor's molecule with active sites on metal surface [10-13]. As a fact, in 2-mercaptobenzimidazole derivatives of 2-(*p*-bromobenzylthio)-1*H*-benzimidazole (Br-BBD) molecular structure, which contain N and S atom as the electronegative atoms, it could be acted as a kind of the potential corrosion inhibitors. As a consequence, the aim of this paper is to describe the adsorption and corrosion inhibition performance of the new synthesized corrosion inhibitor of Br-BBD for Q235 steel in  $\text{HCl}$  solution by EIS, SEM, polarization measurement and WLM (weight loss measurement).

## 2. MATERIALS AND METHODS

### 2.1 Reagents and materials

2-mercaptobenzimidazole and 4-bromobenzyl chloride were purchased from Aladdin Chemistry Co., Ltd., (Shanghai, China). Hydrochloric acid (37%,  $\text{HCl}$ ), sodium carbonate ( $\text{Na}_2\text{CO}_3$ ), acetone and ethanol were purchased from Kelong Chemical Co., Ltd., (Chengdu, China). The working electrode with the working area of  $0.785 \text{ cm}^2$ , all the test samples with the size of  $60 \text{ mm} \times 20 \text{ mm} \times 2 \text{ mm}$ , were prepared by commercially available Q235 steel. Meanwhile, all the different concentration of  $\text{HCl}$  solutions were prepared by distilled water and A. R.  $\text{HCl}$  (37%). During corrosion inhibition performance evaluating process, the temperature of different study solutions was controlled by water thermostat, and all test solutions were open to the air and carried out under static conditions.

### 2.2 Corrosion inhibitor

Synthesis: the investigated corrosion inhibitor of 2-(*p*-bromobenzylthio)-1*H*-benzimidazole (Br-BBD) was synthesized from 2-mercaptobenzimidazole and *p*-bromobenzyl chloride (4-bromobenzyl chloride) according to Figure 1. The specific synthetic route as follows: 2-mercaptobenzimidazole (3.000 g, 0.02 mol) and  $\text{Na}_2\text{CO}_3$  (2.120 g, 0.02 mol) was added in acetone (80 mL) at room temperature. Then *p*-bromobenzyl chloride (4.110 g, 0.02 mol) was dropwise added in the solution for reacting over a period of 50 min. Then the mixture was refluxed for 6.0 h. On completion of this reaction was monitored by thin layer chromatography (TLC). Meanwhile, Br-BBD was purified by recrystallization using ethanol as solvent. After recrystallization, the purified Br-BBD was characterized by elemental analysis, FT-IR spectroscopy and NMR ( $^1\text{H}$ ,  $^{13}\text{C}$ ).

Characterization: Anal. calcd. (Carlo Erba 1106) for  $C_{14}H_{11}BrN_2S$  (%): C 52.68, H 3.47, N 8.78, S 10.04; found C 52.63, H 3.41, N 8.85, S 10.00. FT-IR (Nicolet 6700, KBr,  $cm^{-1}$ ): 3195.4 (w), 3030.0 (w), 2957.0 (m), 2794.7 (m), 1615.4 (w), 1595.7 (m), 1511.2 (w), 1491.0 (m), 1427.4 (m), 1402.5 (vs), 887.8 (m), 827.2 (m).  $^1H$  NMR (Bruker AC-P 400,  $CDCl_3$ , 400 MHz)  $\delta$ : 7.12~7.84 (m, 8H, 2Ar), 4.45 (s, 2H,  $CH_2$ ), 4.43 (s, 1H, NH).  $^{13}C$  NMR (Bruker AC-P 400,  $CDCl_3$ , 100.7 MHz)  $\delta$ : 34.44 ( $CH_2$ ), 115.24~138.75 (2Ar), 149.95 (C=N).

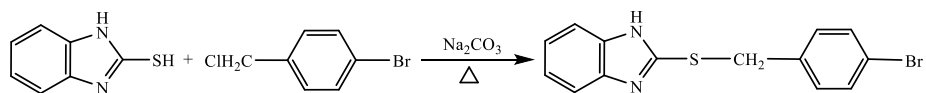


**Figure 1.** Structure and synthetic route of 2-(p-bromobenzylthio)-1H-benzimidazole (Br-BBD)

### 2.3 EIS and polarization measurement

Electrochemical measurements including EIS (electrochemical impedance spectroscopy) and polarization measurement were used to evaluate the corrosion inhibition performance of Br-BBD for Q235 steel in HCl solution, all the electrochemical measurements were controlled by conventional three-electrode system on electrochemical workstation (CHI 660D, Shanghai, China). EIS measurement was performed in frequency range of 10 m Hz to 100 kHz using a sinusoidal AC perturbation with amplitude of 10 mV. The corresponding parameters were fitted by Zsimpwin software, and the inhibition efficiency ( $\eta_{EIS}$ ) derived from EIS was given by Equation 1 [14-17], where  $R_{O_{ct}}$  and  $R_{i_{ct}}$  are the values of charge transfer resistance for Q235 steel in HCl solution without and with different concentrations of Br-BBD, respectively. Meanwhile, according to polarization measurement under the scan rate of  $0.5 \text{ mV s}^{-1}$ , the inhibition efficiency ( $\eta_{Tafel}$ ) described from Equation 2 [18-20], where  $I_0$  and  $I_i$  are the corrosion current density values of Q235 steel in HCl solution without and with different concentrations of Br-BBD, respectively.

$$\eta_{EIS} (\%) = \frac{R_{i_{ct}} - R_{O_{ct}}}{R_{i_{ct}}} \times 100 \quad (1)$$

$$\eta_{Tafel} (\%) = \frac{I_0 - I_i}{I_0} \times 100 \quad (2)$$

### 2.4 WLM

WLM (weight loss measurement) was described in literature [21-24]. The corrosion rate ( $v$ ,  $mg \text{ m}^{-2} \text{ h}^{-1}$ ) and inhibition efficiency ( $\eta_{WLM}$ ) were described by Equation 3 and 4 [21-24], respectively. In Equation 3 and 4,  $m_0$  and  $m_i$  are the mass of the Q235 steel sample before and after immersion in study solution.  $S$  is the total surface area of the Q235 steel sample, which is  $13.6 \text{ cm}^2$ .  $t$  is the test time, which is 12.0 h.  $v_0$  and  $v_i$  are corrosion rate of the Q235 steel corrosion in test solution without and with different concentrations of Br-BBD.

$$v = \frac{m_0 - m_i}{St} \quad (3)$$

$$\eta_{WLM} (\%) = \left(1 - \frac{v_i}{v_0}\right) \times 100 \quad (4)$$

## 2.5 SEM

The SEM (scanning electron microscopy) images of Q235 steel surface before and after corrosion in 1.0 M HCl at 25°C in the absence and presence of Br-BBD for 2.0 hours were examined by Tescan Vega 3 SEM equipped (Czech Republic).

## 3. RESULTS AND DISCUSSION

### 3.1 EIS measurement

Based on EIS method, the Nyquist diagrams for Q235 steel in 1.0 M HCl with different concentrations of Br-BBD at 25°C is shown in Figure 2. Meanwhile, the electrochemical parameters and corresponding inhibition efficiency ( $\eta_{\text{EIS}}$ ) are presented in Table 1.

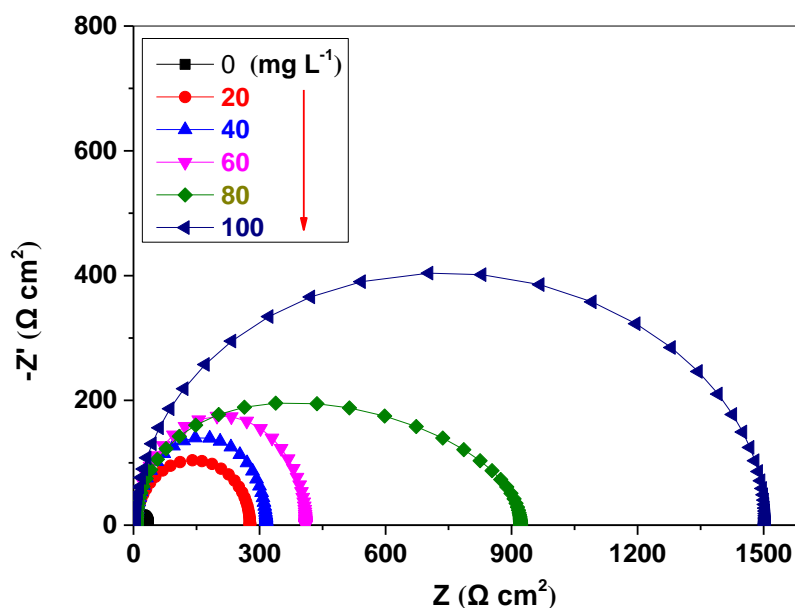


**Figure 2.** Nyquist plots for Q235 steel in 1.0 M HCl with different concentrations of Br-BBD at 25°C

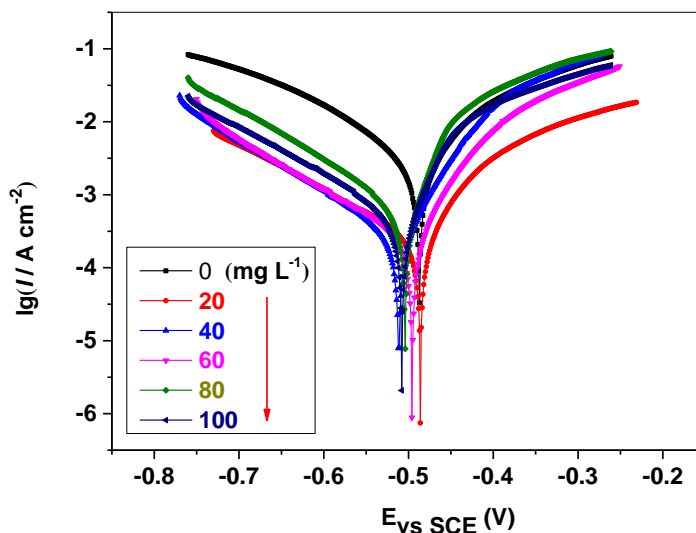
According to Table 1, it can be found that the  $\eta_{\text{EIS}}$  increases with the increase of Br-BBD concentration, and decreases with the increase of double layer capacitance ( $C_{\text{dl}}$ ), it attribute to the gradual replacement of H<sub>2</sub>O molecules resulted from the adsorption of Br-BBD molecules on Q235 steel. The diameter of the capacitive loop increase indicates that the inhibition of the corrosion process of Q235 steel in 1.0 M HCl. The maximum inhibition efficiency recorded by EIS is 98.63% for Q235 steel in 1.0 M HCl with 100 mg L<sup>-1</sup> Br-BBD at 25°C, which shows that Br-BBD can act as an excellent corrosion inhibitor for Q235 steel in HCl solution.

**Table 1.** Electrochemical parameters of impedance and inhibition efficiency for Q235 steel in 1.0 M HCl with different concentrations of Br-BBD at 25°C from EIS measurement

$C_{\text{Br-BBD}} \text{ (mg L}^{-1}\text{)}$	$R_{\text{ict}} \text{ (}\Omega \text{ cm}^2\text{)}$	$C_{\text{dl}} \text{ (}\mu\text{F cm}^{-2}\text{)}$	$\eta_{\text{EIS}} \text{ (\%)}$
0	28.43	50.76	-
20	293.70	28.31	89.74
40	341.30	20.72	90.59
60	403.26	10.21	93.87
80	714.32	8.64	97.13
100	1274.89	6.77	98.63

### 3.2 Polarization measurement

At 25°C, the potentiodynamic polarization curves (Tafel curves) for Q235 steel in 1.0 M HCl with different concentrations of Br-BBD are shown in Figure 3. Meanwhile, the corrosion current density  $I_i$  ( $\mu\text{A cm}^{-2}$ ), corrosion potential  $E_{\text{corr}}$  (mV, vs. SCE) and the corresponding inhibition efficiency ( $\eta_{\text{Tafel}}$ ) calculated by Equation 2 are given in Table 2.

**Figure 3.** Potentiodynamic polarization curves for Q235 steel in 1.0 M HCl with different concentrations of Br-BBD at 25°C

According to Table 2 and Figure 3, it could be found that the anodic and cathodic reactions affected by the addition of Br-BBD. Both the anodic and cathodic curves shift to lower current densities, which indicate that the corrosion inhibitor of Br-BBD can reduce the Q235 steel anodic dissolution in HCl solution. The  $\eta_{\text{Tafel}}$  increases with Br-BBD concentration increasing. A possible inhibition mechanism is the adsorption of Br-BBD molecules on Q235 steel surface through the electronegative atoms including S and N atoms from Br-BBD, which blocks the Q235 steel corrosion in HCl solution. The  $\eta_{\text{Tafel}}$  reaches up to 98.63% when Br-BBD concentration increase to 100 mg L<sup>-1</sup>,

which present that Br-BBD is an effective inhibitor for Q235 steel in HCl solution. The result presented from polarization measurement is in good agreement with it obtained from EIS method. It is clear from Table 2, there is obvious shift towards anodic region in the values of  $E_{corr}$ . The maximum displacement in  $E_{corr}$  value is 17 mV towards anodic region in this study, Based on previous works [25-29], it indicates that the investigated corrosion inhibitor Br-BBD is a mixed-type corrosion inhibitor, and the similar result was reported by Wang [5].

**Table 2.** Polarization parameters and inhibition efficiency for Q235 steel in 1.0 M HCl with different concentrations of Br-BBD at 25°C from polarization measurement

$C_{Br-BBD}$ (mg L <sup>-1</sup> )	$E_{corr}$ (vs SCE, V)	$I_i$ (μA cm <sup>-2</sup> )	$\eta_{Tafel}$ (%)
0	-0.503	1230.30	-
20	-0.507	126.17	89.74
40	-0.509	115.78	90.59
60	-0.511	75.47	93.87
80	-0.496	35.31	97.13
100	-0.486	16.89	98.63

### 3.3 Weight loss measurement

#### 3.3.1 Br-BBD concentration

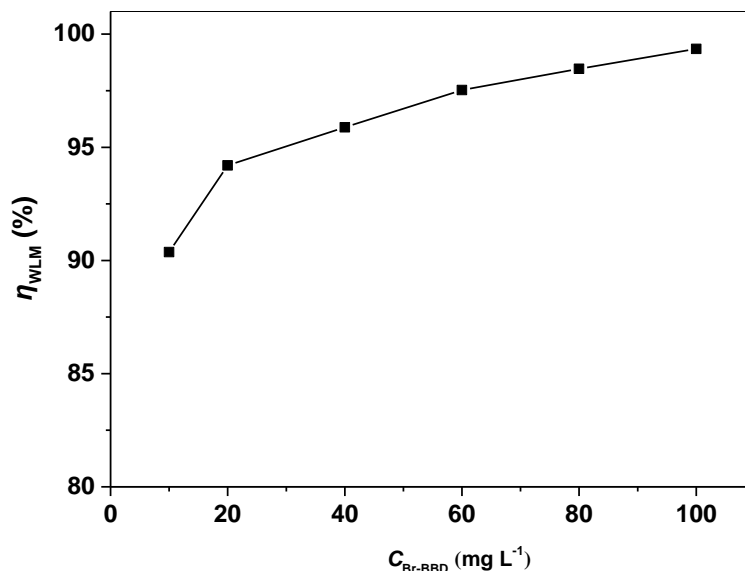


**Figure 4.** The inhibition efficiency for Q235 steel in 1.0 M HCl with different concentrations of Br-BBD at 25°C from WLM method

According to Equation 3 and 4, the inhibition efficiency ( $\eta_{WLM}$ ) for Q235 steel in 1.0 M HCl with different concentrations of Br-BBD at 25°C from WLM (weight loss measurement) is shown in

Figure 4. This Figure shows that the  $\eta_{\text{WLM}}$  has an obvious change with Br-BBD concentration increase from blank solution to  $100 \text{ mg L}^{-1}$ . The  $\eta_{\text{WLM}}$  increase from 90.37% to 99.35% when Br-BBD concentration increase from 10 to  $100 \text{ mg L}^{-1}$ , which confirms that the Br-BBD can act as an effective corrosion inhibitor for Q235 steel in HCl solution. It is a good agreement with EIS and polarization measurement, and all of which present a same trend of Q235 steel corrosion in HCl solution with different concentrations of Br-BBD.

### 3.3.2 Effect of HCl concentration, temperature and storage time

According to WLM method, the impact of HCl concentration, temperature and storage time on inhibition efficiency ( $\eta_{\text{WLM}}$ ) are listed in Table 3. The storage time was defined as the time interval from the time of addition Br-BBD in HCl solution to the time of using the test solution for WLM measurement. In HCl solution with  $100 \text{ mg L}^{-1}$  Br-BBD at  $25^\circ\text{C}$ , it can be found that the  $\eta_{\text{WLM}}$  decreases with HCl concentration increasing, and the minimum  $\eta_{\text{WLM}}$  for Q235 steel in different concentration of HCl solution with  $100 \text{ mg L}^{-1}$  Br-BBD is 93.15% (3.0 M HCl). The decrease of the  $\eta_{\text{WLM}}$  from 99.74% (0.5 M HCl) to 93.15% (3.0 M HCl) is contributed to the increase of  $\text{H}^+$  concentration. Meanwhile, it can be found that the  $\eta_{\text{WLM}}$  also decreases with temperature increasing for Q235 steel in 1.0 M HCl with  $100 \text{ mg L}^{-1}$  Br-BBD. Increase as temperature from  $25^\circ\text{C}$  to  $80^\circ\text{C}$ ,  $\eta_{\text{WLM}}$  has dropped from 99.35% to 51.75%, which sharply decreases for temperature higher than  $60^\circ\text{C}$ . When temperature increases to  $80^\circ\text{C}$ ,  $\eta_{\text{WLM}}$  dropped to 51.75%. Additional, according to the effect of storage time on  $\eta_{\text{WLM}}$ , it can be seen that the  $\eta_{\text{WLM}}$  slightly fluctuates with storage time changing for Q235 steel in 1.0 M HCl with  $100 \text{ mg L}^{-1}$  Br-BBD at  $25^\circ\text{C}$ . At 196 hours later, the  $\eta_{\text{WLM}}$  still up to 99.02%, which shows that Br-BBD still exhibit the excellent corrosion inhibition for Q235 steel in HCl solution for a long time, and further reveals that this inhibitor is a long-acting corrosion inhibitor.

**Table 3.** The effect of HCl concentration, temperature and storage time on inhibition efficiency from WLM method

Factor I $100 \text{ mg L}^{-1}$ Br-BBD $25^\circ\text{C}$		Factor II $100 \text{ mg L}^{-1}$ Br-BBD 1.0 M HCl		Factor III $100 \text{ mg L}^{-1}$ Br-BBD 1.0 M HCl $25^\circ\text{C}$	
<i>HCl</i> <i>concentration</i> (M)	$\eta_{\text{WLM}}$ (%)	<i>Temperature</i> ( $^\circ\text{C}$ )	$\eta_{\text{WLM}}$ (%)	<i>Storage time</i> (h)	$\eta_{\text{WLM}}$ (%)
0.5	99.74	25	99.35	0	99.35
1.0	99.35	40	99.07	24	99.47
1.5	98.36	50	94.86	48	99.31
2.0	97.63	60	87.34	96	99.33
2.5	94.83	70	70.19	144	98.98
3.0	93.15	80	51.71	196	99.02

### 3.3.3 Adsorption isotherm

In this work, in order to identify the adsorption of Br-BBD molecules on Q235 steel surface in HCl solution, the different adsorption isotherms model including Langmuir, Flory–Huggins, Frumkin and Temkin isotherms were suggested to fit using the obtained data in Figure 4 by WLM method. It is obvious that the best adsorption isotherm was determined with Langmuir adsorption isotherm model seen in Equation 5 [30-35], where  $C_{Br-BBD}$  is the concentration of Br-BBD ( $\text{mol L}^{-1}$ ).  $K_{ads}$  is the adsorption equilibrium constant ( $\text{mol L}^{-1}$ )<sup>-1</sup>.  $\theta$  is the surface coverage, which obtained from Equation 6 according to WLM method. The  $v_0$  and  $v$  are corrosion rate ( $\text{mg cm}^{-2} \text{h}^{-1}$ ) of Q235 steel in 1.0 M HCl without and with different concentrations of Br-BBD, respectively.

$$\frac{C_{Br-BBD}}{\theta} = \frac{1}{K_{ads}} + C_{inh} \tag{5}$$

$$\theta = 1 - \frac{v}{v_0} \tag{6}$$

According to Langmuir adsorption isotherm model, the relationships between  $C_{Br-BBD}/\theta$  and  $C_{Br-BBD}$  are shown in Figure 5. From this fitting result, it can be found the adsorption of Br-BBD in HCl solution on Q235 steel surface obeys Langmuir adsorption isotherm ( $R=0.99996$ ). Meanwhile, the  $K_{ads}$  value can be determined from fitting results,  $K_{ads} = M_{Br-BBD} \times K \times 10^3 = (319/1.4121) \times 10^3 = 2.2591 \times 10^5$  ( $\text{mol L}^{-1}$ )<sup>-1</sup>. Where  $M_{Br-BBD}$  is the molar mass of Br-BBD, which is  $319 \text{ g mol}^{-1}$ .  $K$  is the adsorption equilibrium constant ( $(\text{mg L}^{-1})^{-1}$ ). According to  $K_{ads}$ , the standard free energy of adsorption ( $\Delta G_{ads}^0$ ) can be calculated by Equation 7 [30-35], where  $R$  is  $8.314 \text{ J K}^{-1} \text{ mol}^{-1}$ .  $T$  is  $25^\circ\text{C}$  ( $298 \text{ K}$ ). According to Equation 7 and Figure 5, the value of  $\Delta G_{ads}^0$  for Br-BBD in 1.0 M HCl on Q235 steel at  $25^\circ\text{C}$  is  $-40.49 \text{ kJ mol}^{-1}$  ( $< -40 \text{ kJ mol}^{-1}$ ), which presents that the adsorption of Br-BBD in HCl solution on Q235 steel surface is governed by spontaneous chemisorption mechanism.

$$\Delta G_{ads}^0 = -RT \ln (55.5 K_{ads}) \tag{7}$$

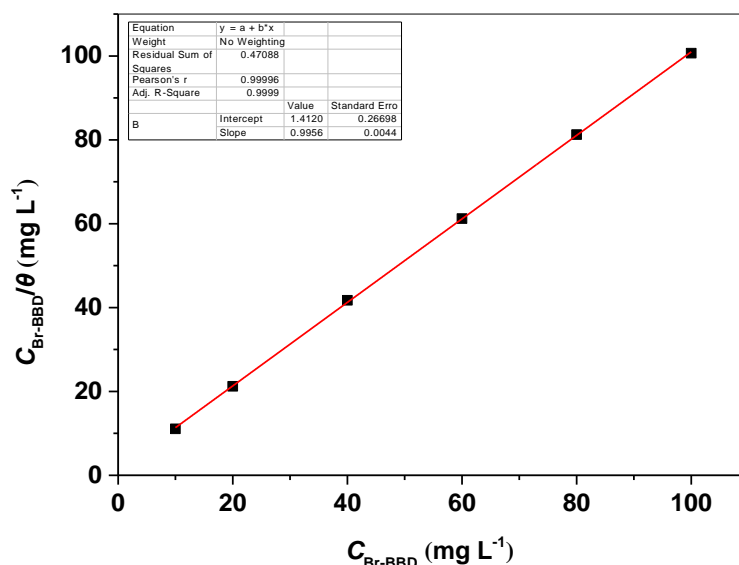


**Figure 5.** Langmuir adsorption isotherm of Br-BBD for Q235 steel in 1.0 M HCl at  $25^\circ\text{C}$  from WLM method



### 3.4 SEM

At 25 °C, the high magnification SEM (scanning electron microscopy) micrographs for Q235 steel surface before and after immersion in 1.0 M HCl without and with 100 mg L<sup>-1</sup> Br-BBD for 2.0 h were shown in Figure 6 (I), (II) and (III), respectively. Figure 6 (I) shows SEM images of Q235 steel sample before immersion in 1.0 M HCl, in which the Q235 steel surface appears more uniform and some abrading scratches.

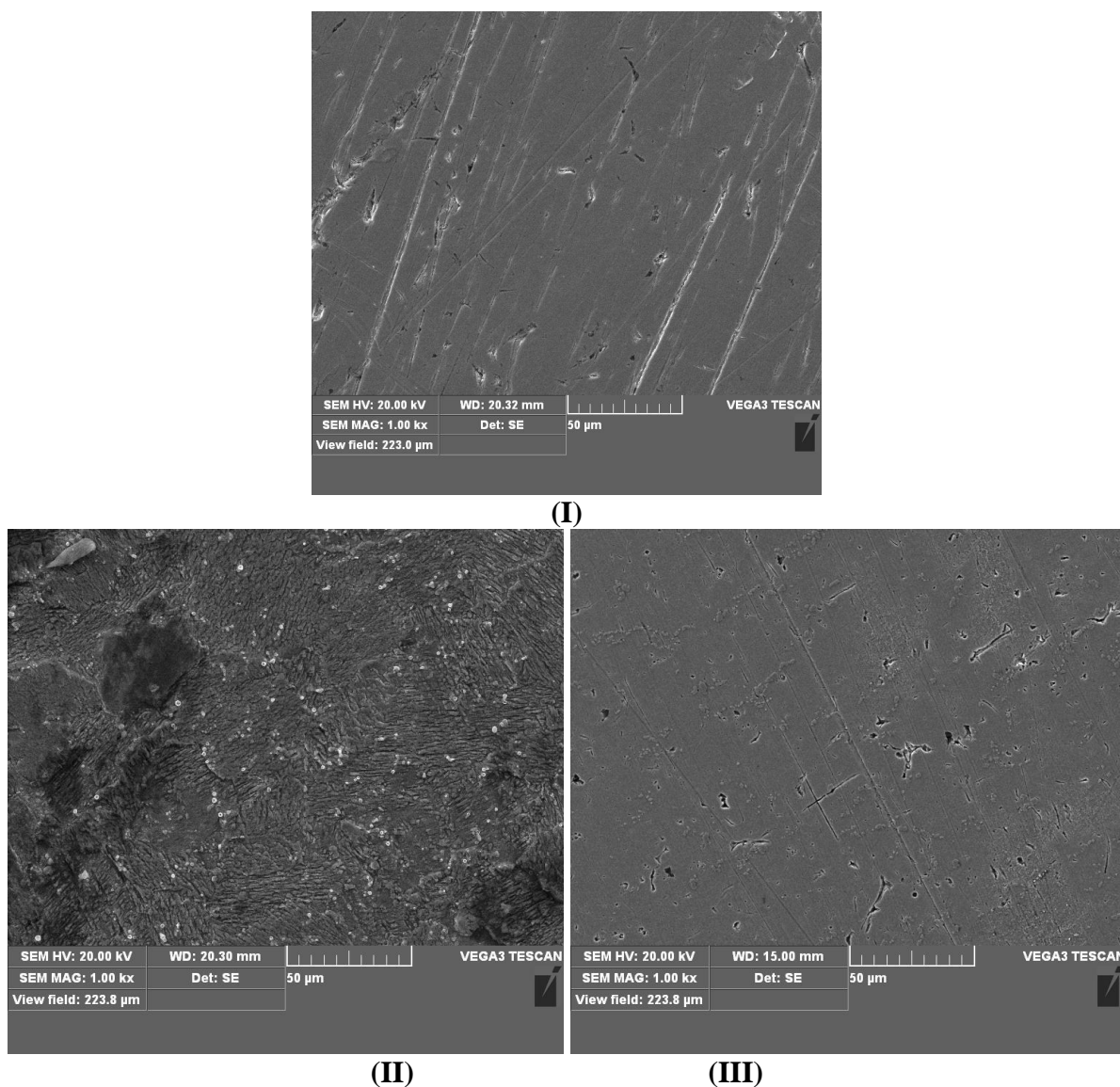


**Figure 6.** SEM micrographs of Q235 steel before (I) and immersion in 1.0 M HCl without (II) and with 100 mg L<sup>-1</sup> Br-BBD (III) at 25 °C for 2.0 h

However, as can be seen from Figure 6 (II), the Q235 steel sample immersion 1.0 M HCl without Br-BBD (blank solution) is deeply corroded and highly damaged, which lead to the surface of Q235 steel becomes too rough and uneven. On the contrary, from Figure 6 (III), in 1.0 M HCl with 100 mg L<sup>-1</sup> Br-BBD, the corrosion degree is suppressed and much less damaged and corroded, which

further confirms the corrosion inhibition of Br-BBD for Q235 steel in HCl solution, which is well-supported by the results from EIS, polarization measurement and WLM method.

#### 4. CONCLUSIONS

In summary, the organic compound of 2-(*p*-bromobenzylthio)-1*H*-benzimidazole (Br-BBD) can act as an excellent new corrosion inhibitor for Q235 steel in HCl solution, and the inhibition efficiency increases with Br-BBD concentration increasing, decreases with temperature and HCl concentration increasing, and slightly fluctuates with storage time changing. This compound is a mixed-type corrosion inhibitor, and the adsorption of the inhibitor on Q235 steel surface is governed by spontaneous chemisorption mechanism and obeys Langmuir adsorption isotherm model. In addition, the corrosion inhibition performance evaluated by EIS, polarization measurement, SEM and WLM method are in good agreement.

#### ACKNOWLEDGMENTS

This project was supported financially by the Projects of Sichuan University of Arts and Science (No. 2015TP002Z), the Project of Zigong City (2012H04), the Program of Education Department of Sichuan Province (No. 16ZA0358), and the Opening Project of Key Laboratory of Green Catalysis of Sichuan Institutes of Higher Education (No LYJ1503).

#### References

1. M. K. Tehrani and A. Niazi, *Int. J. Electrochem. Sci.*, 10 (2015) 6855.
2. S. E. Ayyoubi, A. Chetouani, Hammouti, A. Warthan, A. Mansri and S. S. ADEyab, *Int. J. Electrochem. Sci.*, 7 (2012) 1639.
3. O. O. Xomet, N. V. Likhanova, N. Nava, A. C. Prieto, I. V. Lijanova, A. E. Morales and C. L. Aguila, *Int. J. Electrochem. Sci.*, 9 (2013) 735.
4. N. Yilmaz, A. Fitoz, U. Ergun and K. C. Emregül, *Corros. Sci.*, 111 (2016) 110.
5. L. Wang, J. X. Pu, and H. C. Luo, *Corros. Sci.*, 45 (2003) 677.
6. M. Mahdavian and S. Ashhari, *Electrochim. Acta*, 55 (2010) 1720.
7. L. Wang, *Corros. Sci.*, 43 (2001) 2281.
8. B. Trachli, M. Keddami, H. Takenouti and A. Srhiri, *Prog. Org. Coat.*, 44 (2002) 17.
9. I.B. Obot and N.O. Obi-Egbedi, *Corros. Sci.*, 52 (2010) 657.
10. K.R. Ansari, M.A. Quraishi and A. Singh, *Corros. Sci.*, 95 (2015) 62.
11. A. Popova, M. Christov and A. Vasilev, *Corros. Sci.*, 94 (2015) 70.
12. M. Chellouli, D. Chebabe, A. Dermaj, H. Erramli, N. Bettach, N. Hajjaji, M.P. Casaletto, C. Cirrincione, A. Privitera and A. Srhiri, *Electrochim. Acta*, 204 (2016) 50.
13. Z. A. Abdallah, M. S. M. Ahmed and M.M. Saleh, *Mater. Chem. Phys.*, 174 (2016) 91.
14. P. A. Lozada, O. O. Xomet, N. V. Likhanova, E. M. A. Estrada, I. V. Lijanova, L. L. Rojas and M. C. M. Herrera, *Int. J. Electrochem. Sci.*, 11 (2016) 7785.
15. S. Ben Aoun, M. Bouklah, K.F. Khaled and B. Hammouti, *Int. J. Electrochem. Sci.*, 11 (2016) 7343.
16. M. Bobina, A. Kellenberger, J.P. Millet, C. Muntean and N. Vaszilcsin, *Corros. Sci.*, 69 (2013) 389.
17. K.K. Anupama, K. Ramya, K.M. Shainy and A. Joseph, *Mater. Chem. Phys.*, 167 (2015) 28.

18. A. Zarrouk, B. Hammouti, T. Lakhelifi, M. Traisnel, H. Vezin and F. Bentiss, *Corros. Sci.*, 90 (2015) 572.
19. A. Biswas, S. Pal and G. Udayabhanu, *Appl. Surf. Sci.*, 353 (2015) 173.
20. I. B. Obot and A. Madhankumar, *Mater. Chem. Phys.*, 177 (2016) 266.
21. R. Yıldız, *Corros. Sci.*, 90 (2015) 544.
22. X. Ma, X. Jiang, S. Xia, M. Shan, X. Li, L. Yu and Q. Tang, *Appl. Surf. Sci.*, 371 (2016) 284.
23. M. A. Chidiebere, E. E. Oguzie, L. Liu, Y. Li and F. Wang, *Mater. Chem. Phys.*, 156 (2015) 95.
24. M. Farsak, H. Keleş and M. Keleş, *Corros. Sci.*, 98 (2015) 223.
25. M. Chevalier, F. Robert, N. Amusant, M. Traisnel, C. Roos and M. Lebrini *Electrochim. Acta*, 131 (2014) 96.
26. P. B. Raja, A. K. Qureshi, A. A. Rahim, H. Osman and K. Awang, *Corros. Sci.*, 69 (2013) 292.
27. D. B. Hmamou, A. Zarrouk, R. Salghi, H. Zarrok, E. E. Ebenso, B. Hammouti, M. M. Kabanda, N. Benchat and O. Benali, *Int. J. Electrochem. Sci.*, 9 (2014) 120.
28. R. Yıldız, A. Döner, T. Doğan and I. Dehri, *Corros. Sci.*, 82 (2014) 125.
29. G. I. Ostapenko, P. A. Gloukhov and A. S. Bunev, *Corros. Sci.*, 82 (2014) 265.
30. N. E. Hamdani, R. Fdil, M. Tourabi, C. Jama and F. Bentiss, *Appl. Surf. Sci.*, 357 (2015) 1294.
31. I. Lozano, E. Mazario, C.O. Olivares-Xometl, N.V. Likhanova and P. Herrasti, *Mater. Chem. Phys.*, 147 (2014) 191.
32. A. E. Bribri, M. Tabyaoui, B. Tabyaoui, H. E. Attari and F. Bentiss, *Mater. Chem. Phys.*, 141 (2013) 240.
33. H. Cang, Z. Fei, J. Shao, W. Shi and Q. Xu, *Int. J. Electrochem. Sci.*, 9 (2013) 720.
34. A. U. Ezeoke, O. G. Adeyemi, O. A. Akerele and N. O. Obi-Egbedi, *Int. J. Electrochem. Sci.*, 8 (2012) 534.
35. D. B. Hmamou, R. Salghi, L. Bazzi, B. Hammouti, S. S. A. Deyab, L. Bammou, L. Bazzi and A. Bouyanze, *Int. J. Electrochem. Sci.*, 7 (2012) 1303.